UNIVERSITÀ DEGLI STUDI DI PALERMO

Dottorato di Ricerca in Medicina del Benessere, Nutrigenomica e Malattie Degenerative
Dipartimento Biomedico di Medicina Interna e Specialistica (DIBIMIS)
SSD: MED-36

Université de Paris

École doctorale Médicament, Toxicologie, Chimie, Imageries (ED 563)
Prof. Marie-Christine Lallemand
Prof. Armelle Baeza

Long-term evolution of hepatocellular adenomas

at MRI follow-up

THE DOCTOR
FEDERICA VERNUCCIO

THE COORDINATOR
PROF. ANTONIO PINTO

THE TUTOR
PROF. GIUSEPPE BRANCATELLI

THE CO-TUROR
PROF. VALERIE VILGRAIN

CICLO XXXIII
ANNO ACCADEMICO/ACADEMIC YEAR 2019/2020

UNIVERSITÀ DEGLI STUDI DI PALERMO

Université de Paris

Index

To my parents, I owe you

Part 1- Hepatocellular Adenomas

1.1 Introduction

Hepatocellular adenomas (HCA) occur in three to four per 100 000 people in the general population [1], mainly in young women. Risk factors for HCAs include oral contraceptive and anabolic steroid [2-7]. Prolonged oral contraceptive use is associated with the presence of multiple adenomas and the term adenomatosis refers to the presence of more of 10 HCAs at pathology [8, 9].

HCAs are subclassified into different subtypes based on the molecular/genetic characteristics, including HCAs inactivated for HNF1A, inflammatory HCAs, β-catenin-activated HCAs mutated in exon 3, β-catenin-activated HCAs mutated in exon 7–8, sonic hedgehog HCAs, and unclassified HCAs [8-12]. Multimodality imaging, with a combined approach through ultrasound (US), contrast enhanced ultrasound (CEUS) and Magnetic Resonance Imaging (MRI) is effective in characterizing HNF1α-mutated and inflammatory HCAs. MRI features of the four main subtypes of HCAs are shown in **Table 1**.

	HNF1α-mutated	β-catenin mutated	Inflammatory-telangiectatic	Unclassified
Steatotic background liver parenchyma	0-20%	0-17%	24-76%	0-20%
Diffuse intra-lesional fat	78-80%	0%	0-10%	0%
Hyperintensity on T2WI	30-100%	33-50%	81-83%	33-40%
Atoll sign	0%	0%	38-43%	0%
Marked APHE	10-33%	0-33%	48-86%	20-33%
Washout on PVP	70-100%	17%	5-8%	12-33%
Hypointensity in HBP	100%	17%	71-91%	75-100%

Table 1 MRI features of main subtypes of hepatocellular adenomas. T2WI: T2-weighted images; APHE: arterial phase hyperenhancement; PVP: portal venous phase; HBP: hepatobiliary phase.

Complications (i.e. spontaneous hemorrhage (**Figure 1**) and malignant transformation) may occur, particularly depending on male gender, tumor size and HCA subtype [13-15]. Indeed, malignant transformation is more common in HCAs with mutations of the ß-catenin gene [16,17], while sonic hedgehog HCAs seem at higher risk of hemorrhage compared to other subtypes. Therefore, the management of HCAs depends on several factors.

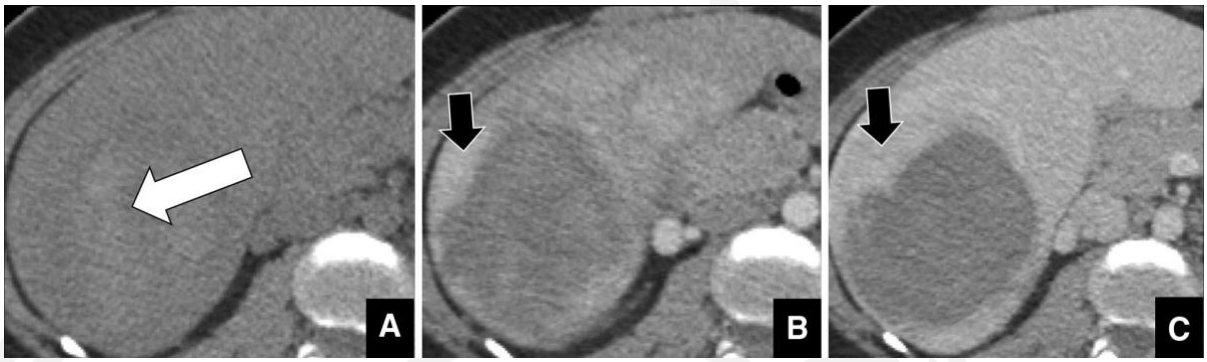

Fig. 1 - Hemorrhagic and necrotic HCA in a 35-year-old woman with history of oral contraceptives intake for 12 years who complained of abdominal pain after oral intake of nonsteroidal anti-inflammatory drugs. Axial CT images on (A) unenhanced, (B) arterial and (C) portal phases show a spontaneously hyperattenuating liver lesion in the right lobe (white arrow), with mild peripheral enhancement (black arrows) without any enhancement of the central core. Patient underwent right hepatectomy with diagnosis of inflammatory HCA with hemorrhagic and necrotic foci.

1.2 Hepatocyte Nuclear Factor 1α-Mutated Hepatocellular Adenomas

Hepatocyte nuclear factor 1α (HNF1α)-mutated HCAs, also known as steatotic HCA, constitute about 27 to 36% of all HCAs [9,10,13]. HNF1α-mutated HCAs have a bi-allelic mutation of the TCF1 gene inactivating the HNF1α transcription factor. At pathology, it is characterized by marked steatosis and lack of cytological abnormalities and inflammatory infiltrate (**Figure 2**). Immunohistochemistry shows that these HNF1α-mutated HCAs lack staining of the liver fatty acid binding protein (L-FABP), that is instead highly expressed in the non-tumoral liver [9,13,18,19].

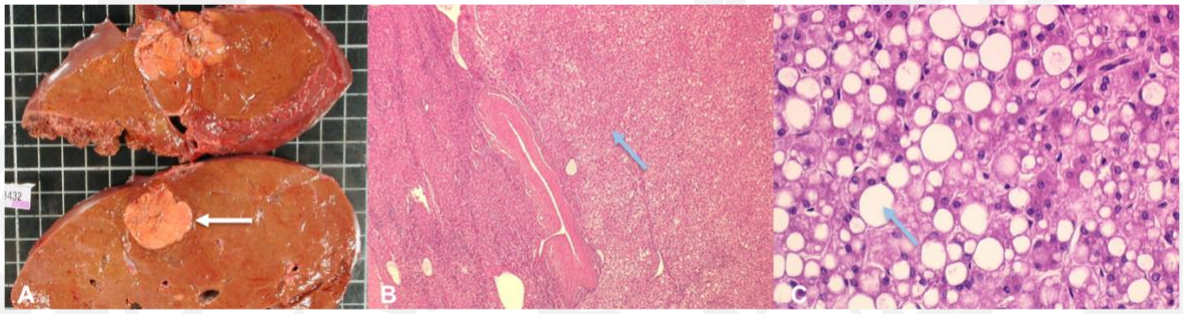

Fig. 2: 46-year-old woman with HNF1α-mutated HCA. A, Photograph of fresh resected specimen shows a well-defined homogeneous tumor (white arrow). B and C, Photomicrograph shows marked and diffuse steatosis (blue arrows).

The key imaging feature of HNF1α-mutated HCAs is the presence of marked and diffuse fat within the lesion:

- on US: HNF1α-mutated HCAs are homogeneous and strongly hyperechoic lesions on B-mode, with discrete or lack of enhancement on CEUS; when enhancement is present, it shows a centripetal or mixed arterial filling, and it is isoechoic on portal and delayed phases[20-22].
- On CT, HNF1α-mutated HCAs show marked low attenuation on unenhanced phase, mild or lack of enhancement on arterial phase and wash-out on portal or delayed phases.

- On MRI, HNF1α-mutated HCAs are usually slightly hyperintense on non-fat suppressed T2-weighted sequence and iso-or hypointense on fat suppressed T2-weighted sequence, with diffuse and homogeneous signal drop on opposed phase and hypointensity in the hepatobiliary phase (**Figure 3**) [23-28]. Among all HCAs, HNF1α-mutated subtype is the least aggressive [23]; therefore conservative management is usually indicated [13,15, 29].

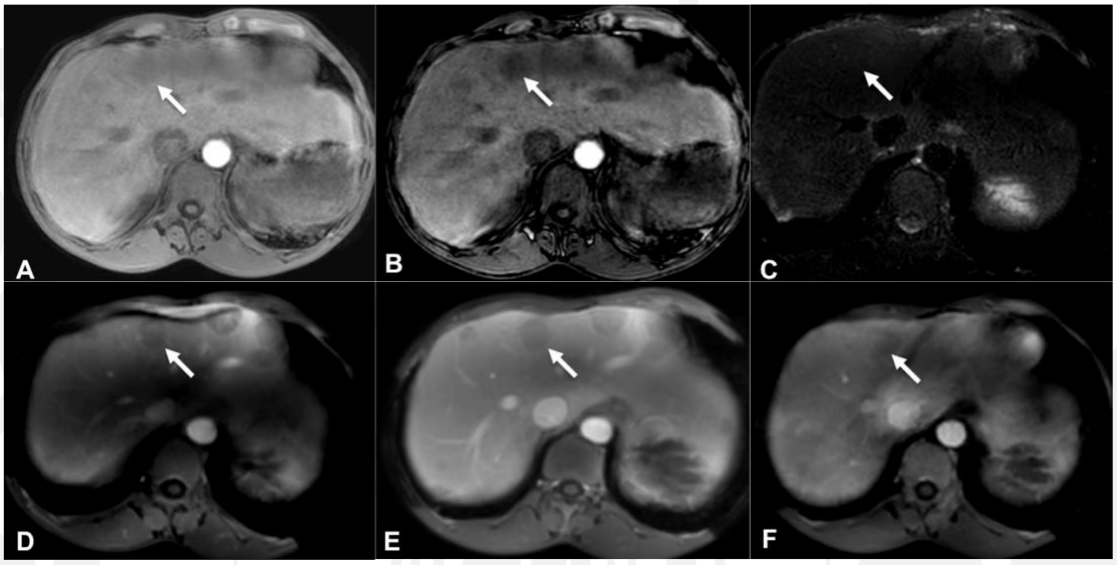

Fig. 3 38-year-old woman with HNF1α-mutated HCA (white arrow). MRI. In-phase (A) and opposed-phase (B) T1-weighted images show a strong and homogenous signal drop of due to marked fat content. (C) On respiratory-triggered fat-suppressed turbo spin-echo T2-weighted imaging, the lesion is isointense compared to the surrounding liver. On 3D fat-suppressed GRE T1-weighted acquisitions after intravenous injection of gadoxetic acid, the lesion shows slight enhancement on arterial phase imaging (D). On portal venous (E) delayed phases (F) the lesion is hypointense.

1.3 Inflammatory HCAs

Inflammatory HCAs account for up to 46-54% of all HCAs [9, 10,13]. These HCAs are commonly observed in women on oral contraceptive, but are also associated with increased body mass index and inflammatory syndrome [30].

At pathology, the hepatocellular proliferation contains areas of vascular changes (i.e. sinusoidal dilatation and/or peliotic changes), few and short fibrous septa around clusters of small vessels, sometimes accompanied by inflammatory infiltrates, a relatively low degree of ductular reaction, and lack of evident fibrous scar (**Figure 4**). Steatosis may be observed in the lesion or in the nontumoral parenchyma with various degrees of intensity. Inflammatory HCAs are defined by JAK/STAT pathway activation and immunostaining is positive for acute phase inflammatory proteins such as serum amyloid A (SAA) and CRP [9,12,13,18,19]. Approximately 10% of inflammatory HCAs have a β-catenin activation, which is considered to promote their malignant transformation [12].

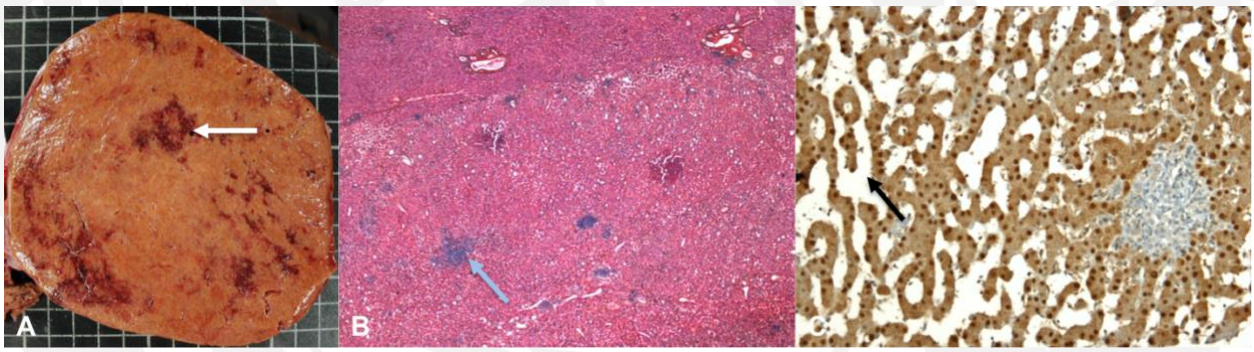

Fig. 4 - 43-year-old obese woman with inflammatory HCA. A, Photograph of fresh resected specimen shows areas of focal hemorrhage inside the tumor (white arrow). B and C, Photomicrograph shows clusters of small arteries surrounded by focal inflammation (blue arrow), and hepatocytes arranged in thin plates separated by dilated sinusoids (black arrow).

The key imaging features of inflammatory HCAs are related to the presence of telangiectatic changes within the tumor:

- On US, the lesion is well delineated, often hyperechoic and heterogeneous [23, 24]; On CEUS, inflammatory HCAs are strongly hypervascular in the arterial phase with centripetal enhancement filing and peripheral linear vascularities in the early phase of filling. In the late portal venous phase, peripheral rim of sustained enhancement with central washout is common [21, 24].
- On CT, inflammatory HCAs are spontaneously hypoattenuating and heterogeneous, with strong arterial enhancement (93%) and a persistent enhancement in the delayed phase (96%) [27]. Foci of bleeding may be also observed on unenhanced phase.
- on MRI these lesions are usually hyperintense on T2-weighted images (either diffuse or as a rim-like band in the periphery of the lesion defined as the atoll sign) [31]. Heterogeneous fat within the lesion may be also encountered but it should not be confused with the marked and homogeneous fat seen in HNF1a-mutated HCAs. Contrast enhancement behavior in extracellular phases is similar to that on CT with strong arterial enhancement that persist in the delayed phases (**Figure 5**). In the hepatobiliary phase most inflammatory HCAs are hypointense compared to the background liver [25-27], but some of them can display a relative hyperintense signal due to common hyperintensity on precontrast images [32, 33]. Inflammatory HCAs are more prone to bleeding compared to HNF1a-mutated HCAs, and show an increased risk for malignancy. Surgical resection or close follow-up, depending on the lesion size, gender and the ß-catenin status, is recommended [13, 15, 17, 29].

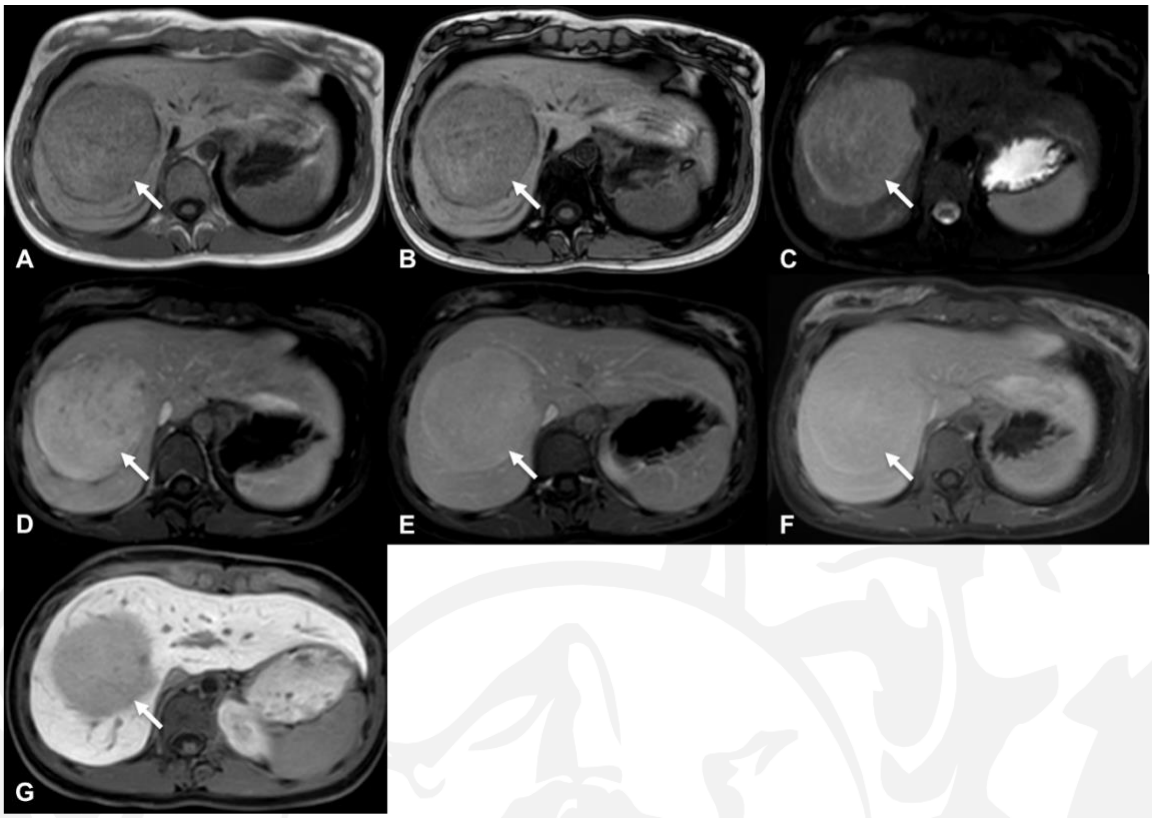

Fig. 5 - 35-year-old woman with inflammatory HCA (white arrow). MRI. In-phase (A) and opposed-phase (B) T1-weighted gradient-echo sequence showing moderate-low intensity without any signal drop on opposed phase. (C) On respiratory-triggered fat-suppressed turbo spin-echo T2-weighted imaging, the lesion is hyperintense compared to the surrounding liver. 3D fat-suppressed gradient-echo T1-weighted acquisitions after intravenous injection of gadolinium chelate (gadoxetic acid): the lesion shows a strong homogenous enhancement on arterial phase imaging (D), with persistent enhancement on portal venous (E) and delayed phases (F). On hepatobiliary phase (G), the lesion is hypointense.

1.4 ß-catenin activated exon 3 and exon 7, Sonic hedgehog, and unclassified HCAs

ß-catenin subtype accounts for 8 to 12.5% of HCAs, including about 7% of ß-catenin exon 3 and about 3% of ß-catenin exon 7 or 8 [9,10,13]. ß-catenin exon 3 HCAs are mostly encountered in men and frequently show cellular atypia and pseudoglandular formation. On immunochemistry, β-catenin-mutated HCA exon 3 is defined by nuclear translocation of β-catenin and overexpression of glutamine synthase, a target gene of the pathway. Risk of malignant transformation in HCC of ß-catenin exon 3 HCAs attains 40%.

In ß-catenin mutated HCAs exon 7 or 8, the mutations lead to mild activation of the Wnt/β-catenin pathway. At histology and immunochemistry, there are no specific markers and this subtype has not been associated with higher risk of malignant transformation.

Unclassified HCAs represent about 7% of all HCAs and correspond to HCAs without specific pathologic abnormalities with lack of distinct genetic alterations or imaging characteristics.

Sonic hedgehog HCAs have recently been recognized and represent 4% of all HCAs [12]. This subtype is defined by activation of the sonic hedgehog pathway due to fusion of the promoter of INHBE with GLI1 and is associated with obesity, and with both histological hemorrhage and symptomatic bleeding.

These subtypes are less characteristic at imaging. The most relevant feature is that most ß-catenin activated HCAs exon 3 show iso or hyperintensity in the hepatobiliary phase of gadoxetic acid–enhanced MRI, but this feature might also be observed in inflammatory HCAs [32-36].

1.5 References

1. Rooks JB, Ory HW, Ishak KG, et al. Epidemiology of hepatocellular adenoma. The role of oral contraceptive use. JAMA. 1979; 242:644-648.
2. Edmondson HA, Henderson B, Benton B. Liver-cell adenomas associated with use of oral contraceptives. N Engl J Med. 1976; 294:470-472.
3. Sale GE, Lerner KG. Multiple tumors after androgen therapy. Arch Pathol Lab Med. 1977; 101:600-603.
4. Labrune P, Trioche P, Duvaltier I, Chevalier P, Odièvre M. Hepatocellular adenomas in glycogen storage disease type I and III: a series of 43 patients and review of the literature. J Pediatr Gastroenterol Nutr. 1997; 24:276-279.
5. Lee P, Mather S, Owens C, Leonard J, Dicks-Mireaux C. Hepatic ultrasound findings in the glycogen storage diseases. Br J Radiol. 1994; 67:1062-1066.
6. Dokmak S, Belghiti J. Will weight loss become a future treatment of hepatocellular adenoma in obese patients?. Liver Int. 2015; 35:2228-2232.
7. Zucman-Rossi J, Jeannot E, Nhieu JT, et al. Genotype-phenotype correlation in hepatocellular adenoma: new classification and relationship with HCC. Hepatology. 2006; 43:515-524.
8. Flejou JF, Barge J, Menu Y, et al. Liver adenomatosis. An entity distinct from liver adenoma?. Gastroenterology. 1985; 89:1132-1138.
9. Bioulac-Sage P, Balabaud C, Bedossa P, et al. Pathological diagnosis of liver cell adenoma and focal nodular hyperplasia: Bordeaux update. J Hepatol. 2007; 46:521-527.
10. Bioulac-Sage P, Rebouissou S, Thomas C, et al. Hepatocellular adenoma subtype classification using molecular markers and immunohistochemistry. Hepatology. 2007; 46:740-748.
11. Bioulac-Sage P, Cubel G, Taouji S, et al. Immunohistochemical markers on needle biopsies are helpful for the diagnosis of focal nodular hyperplasia and hepatocellular adenoma subtypes. Am J Surg Pathol. 2012; 36:1691-1699.

12. Nault JC, Couchy G, Balabaud C, et al. Molecular Classification of Hepatocellular Adenoma Associates With Risk Factors, Bleeding, and Malignant Transformation. Gastroenterology. 2017; 152:880-894.e6.
13. Dokmak S, Paradis V, Vilgrain V, et al. A single-center surgical experience of 122 patients with single and multiple hepatocellular adenomas. Gastroenterology. 2009; 137:1698-1705.
14. van Aalten SM, de Man RA, IJzermans JN, Terkivatan T. Systematic review of haemorrhage and rupture of hepatocellular adenomas. Br J Surg. 2012; 99:911-916.
15. Laurent A, Dokmak S, Nault JC, et al. European experience of 573 liver resections for hepatocellular adenoma: a cross-sectional study by the AFC-HCA-2013 study group. HPB (Oxford). 2016; 18:748-755.
16. Monga SP. Hepatic adenomas: presumed innocent until proven to be beta-catenin mutated. Hepatology. 2006; 43:401-404.
17. Van der Borght S, Libbrecht L, Katoonizadeh A, et al. Nuclear beta-catenin staining and absence of steatosis are indicators of hepatocellular adenomas with an increased risk of malignancy. Histopathology. 2007; 51:855-856.
18. Bioulac-Sage P, Laumonier H, Couchy G, et al. Hepatocellular adenoma management and phenotypic classification: the Bordeaux experience. Hepatology. 2009; 50:481-489.
19. Dhingra S, Fiel MI. Update on the new classification of hepatic adenomas: clinical, molecular, and pathologic characteristics. Arch Pathol Lab Med. 2014; 138:1090-1097.
20. Laumonier H, Cailliez H, Balabaud C, et al. Role of contrast-enhanced sonography in differentiation of subtypes of hepatocellular adenoma: correlation with MRI findings. AJR Am J Roentgenol. 2012; 199:341-348.
21. Soussan M, Aubé C, Bahrami S, Boursier J, Valla DC, Vilgrain V. Incidental focal solid liver lesions: diagnostic performance of contrast-enhanced ultrasound and MR imaging. Eur Radiol. 2010; 20:1715-1725.
22. Gregory J, Paisant A, Paulatto L, et al. Limited added value of contrast-enhanced ultrasound over B-mode for the subtyping of hepatocellular adenomas. Eur J Radiol. 2020 Jul;128:109027.

23. Ronot M, Bahrami S, Calderaro J, et al. Hepatocellular adenomas: accuracy of magnetic resonance imaging and liver biopsy in subtype classification [published correction appears in Hepatology. 2011; 54:1114. Belghti, Jacques [corrected to Belghiti, Jacques]]. Hepatology. 2011; 53:1182-1191.
24. Laumonier H, Bioulac-Sage P, Laurent C, Zucman-Rossi J, Balabaud C, Trillaud H. Hepatocellular adenomas: magnetic resonance imaging features as a function of molecular pathological classification [published correction appears in Hepatology. 2008; 48:1356]. Hepatology. 2008; 48:808-818.
25. Manichon AF, Bancel B, Durieux-Millon M, et al. Hepatocellular adenoma: evaluation with contrast-enhanced ultrasound and MRI and correlation with pathologic and phenotypic classification in 26 lesions. HPB Surg. 2012;2012:418745.
26. Grazioli L, Bondioni MP, Haradome H, et al. Hepatocellular adenoma and focal nodular hyperplasia: value of gadoxetic acid-enhanced MR imaging in differential diagnosis. Radiology. 2012; 262:520-529.
27. Tse JR, Naini BV, Lu DS, Raman SS. Qualitative and Quantitative Gadoxetic Acid-enhanced MR Imaging Helps Subtype Hepatocellular Adenomas. Radiology. 2016; 279:118-127.
28. Yoneda N, Matsui O, Kitao A, et al. Benign Hepatocellular Nodules: Hepatobiliary Phase of Gadoxetic Acid-enhanced MR Imaging Based on Molecular Background. Radiographics. 2016; 36:2010-2027.
29. van Aalten SM, Witjes CD, de Man RA, Ijzermans JN, Terkivatan T. Can a decision-making model be justified in the management of hepatocellular adenoma?. Liver Int. 2012; 32:28-37.
30. Paradis V, Champault A, Ronot M, et al. Telangiectatic adenoma: an entity associated with increased body mass index and inflammation. Hepatology. 2007; 46:140-146.
31. van Aalten SM, Thomeer MG, Terkivatan T, Dwarkasing RS, Verheij J, de Man RA, Ijzermans JN. Hepatocellular adenomas: correlation of MR imaging findings with pathologic subtype classification. Radiology. 2011; 261:172-81.

32. Agarwal S, Fuentes-Orrego JM, Arnason T, Misdraji J, Jhaveri KS, Harisinghani M, Hahn PF. Inflammatory hepatocellular adenomas can mimic focal nodular hyperplasia on gadoxetic acid-enhanced MRI. AJR Am J Roentgenol. 2014; 203:W408-14.
33. Fukusato T, Soejima Y, Kondo F, et al. Preserved or enhanced OATP1B3 expression in hepatocellular adenoma subtypes with nuclear accumulation of β-catenin. Hepatol Res. 2015; 45:E32-E42.
34. Reizine E, Ronot M, Pigneur F, et al. Iso- or hyperintensity of hepatocellular adenomas on hepatobiliary phase does not always correspond to hepatospecific contrast-agent uptake: importance for tumor subtyping. Eur Radiol. 2019;29(7):3791-3801.
35. Yoneda N, Matsui O, Kitao A, et al. Beta-catenin-activated hepatocellular adenoma showing hyperintensity on hepatobiliary-phase gadoxetic-enhanced magnetic resonance imaging and overexpression of OATP8. Jpn J Radiol. 2012; 30:777-782.
36. Reizine E, Ronot M, Ghosn M, et al. Hepatospecific MR contrast agent uptake on hepatobiliary phase can be used as a biomarker of marked β-catenin activation in hepatocellular adenoma. Eur Radiol. 2020 Nov 4. doi: 10.1007/s00330-020-07434-z

PART 2 – Original Research: Long-term evolution of hepatocellular adenomas at MRI follow-up

2.1 Introduction

Hepatocellular adenomas (HCAs) are rare benign liver tumors, which occur in 0.001–0.004% of the population and typically affect young women (10:1 female to male ratio) [1-3]. These tumors may be complicated by hemorrhage or malignant transformation in up to 27% and 4% of affected patients, respectively [4, 5]. Tumor size increase is considered one of the risk factors for complications [4, 5]. It is known that HCAs may progress both in size and number over time, potentially placing patients at risk for complications. Therefore, European Association for the Study of the Liver (EASL) guidelines recommend surveillance with MRI every six months for the first year after diagnosis of HCAs and then annually, as well as lesion resection for tumors that continue to grow or larger than 50 mm [1].

The time points for lesion follow-up according to EASL guidelines are mainly based on small studies or expert opinion, rather than solid evidence. Indeed, it is known that progression of HCAs may occur in up to 19% of patients [6-16] and that size changes could correlate with different patient- and lesion-related variables [14-16]. However, prior studies were limited by small number of patients, relatively short overall follow-up, lack of HCA subtyping and, above all, lack of consistent use of MRI for lesion follow-up. MRI is preferred over CT by EASL guidelines for HCA imaging follow-up not only for the lack of exposure to ionizing radiation, but also because of its high soft tissue resolution and its multiparametric nature, both of which may result in higher diagnostic accuracy for HCA detection, characterization

and subtyping [17]. To date, there are few longitudinal analytical studies on long-term MRI follow-up of HCAs. An evidence based understanding of the natural history of different subtypes of HCAs on MRI may help to inform patient-tailored recommendations, which in turn may result in better patient management and outcome.

The primary aim of this study was to analyze the long-term evolution of different subtypes of HCAs. Secondary aims included determining if there were difference in natural history between solitary and multiple lesions and to identify predictive features of progression.

2.2 Materials and Methods

This retrospective, single-center, cohort study was approved by Institutional Review Board of Beaujon Hospital in Clichy, France – tertiary referral center for liver diseases – and a waiver of written informed consent was obtained. Patients that were joined for the telephone interview were consented orally.

Study cohort

Figure 1 portrays the patients' accrual flowchart, which was based on Strengthening the Reporting of Observational Studies in Epidemiology, or STROBE guidelines [18].

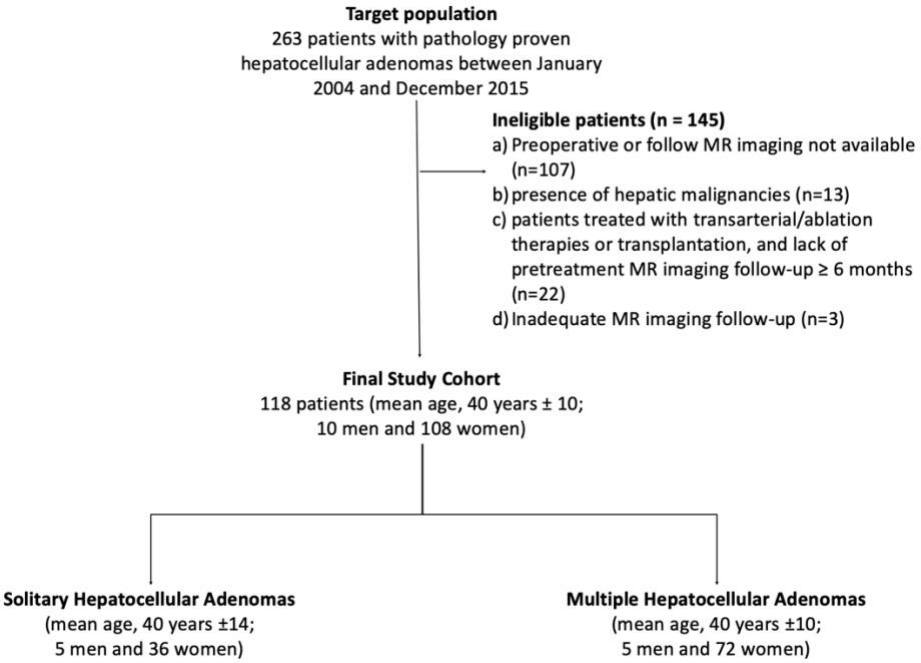

Fig. 1 – Flowchart shows study enrollment based on recommended Standards for Reporting of Diagnostic Accuracy criteria, as well as the reference standard.

We retrospectively searched our Departmental database at Beaujon Hospital in Clichy, France for consecutive patients diagnosed with pathology-proven (i.e., biopsy or surgery) solitary and multiple HCAs between January 2004 and December 2015. Patients were excluded if (a) preoperative or follow-up MRI was not available – including lack of a minimum overall follow-up of 6 months (b) presence of hepatic malignancies (e.g. HCC, metastases) which could potentially have an influence on the natural evolution of HCAs; (c) patients treated with locoregional therapies (i.e. transarterial embolization, radiofrequency ablation) or transplantation,; (d) inadequate MRI protocol. MRI protocol was considered

inadequate if the following key MRI sequences were missing or non-diagnostic: (i) fat saturated T2-weighted sequence, (ii) dual phase sequence, (iii) fat saturated T1-weighted sequence before and after i.v. contrast administration.

Clinical data

We reviewed the electronic records for the included patients and assessed demographic information for each patient, notably age and sex. Then, we performed a telephone interview to collect the following patient related factors: symptoms at diagnosis, height and weight at diagnosis, diabetes, hypercholesterolemia, arterial hypertension, use of oral contraceptives – including age at initial intake and interruption – age of menarche, menopause, and history of pregnancies. Height and weight were used to calculate the body mass index [15]. Time on oral contraceptive before diagnosis was calculated as the difference between age at interruption and age at first intake of the therapy. As the standard-of-care, all women with a diagnosis of HCAs had stopped the use of oral contraceptives.

Reference Standard

All specimens were reviewed by an experienced hepatobiliary pathologist (V.P., with 25 years of experience, who was blinded to clinical information, imaging test results and original pathology report). The following information was assessed for each patient: (a) aspect of non-tumoral liver (fibrosis and steatosis, including the percentage of steatosis, and the presence of microadenomas in resected specimen [i.e. microscopic foci of adenomas less than 1 cm undetected on preoperative radiologic imaging]); (b) subtype of HCA

according to the updated classification published by Nault et al [4], including inflammatory, HNF-1α inactivated, ß-catenin mutated (in exon 3 or in exon 7-8), sonic Hedgehog and unclassified HCAs (see Supplementary Data File); (c) micro- and/or macroscopic hemorrhage within the lesion; (d) malignant foci within the lesion. Malignancy within the lesion was diagnosed when pathologic examination revealed foci of hepatocellular carcinoma inside the adenomatous proliferation. Pathology proof of HCA was biopsy in 32 patients, surgery in 86 patients. At pathology, lesion characteristics (i.e., subtype, hemorrhage or malignancy within the lesion) were available for all of the 41 patients with solitary HCA, and in 129 lesions in the 77 patients with multiple HCAs, while characteristics of non-tumoral liver were available in 95 patients, including 38 patients with solitary HCA and 57 with multiple HCAs. MRI findings were used for subtype classification of HCAs without pathologic proof in patients with multiple HCAs (55.9%, 166/297) and the newly developed HCAs after surgery. Specifically, MRI sequences used to subtype HCAs were T2 weighted-, in- and opposed phase, multiphasic contrast-enhanced sequences during late arterial, portal venous, and delayed phases according to the reference papers [19,20]. MRI signal features that allowed the identification of HCA subtypes at imaging are described in the **Supplementary Data**. HCAs were defined as “at-risk of progression” in case of presence of ß-catenin mutation in exon 3 or presence foci of malignancy on resected tumors.

MRI Analysis

Using the institutions' picture archiving and communication systems (Carestream PACS, version 12.1.5.6009; Kodak, Rochester, NY), MRI exams were reviewed according to Response Evaluation Criteria In Solid Tumors (RECIST) version 1.1 by two radiologists in consensus (F.V. and V.V., with six years and thirty-two years of experience in liver imaging, respectively) who were blinded to the original radiology report, but not to the pathology results of the lesions[21]. Time points for MRI follow-up had been performed at the discretion of the treating physician or based on patients' symptoms. Further information are provided in the **Supplementary Data**. In patients with multiple HCAs, in addition to the surgically resected HCAs (n=88) evaluated at baseline MRI, maximum of three target lesions per subtype per patient – for a total of 209 lesions – were analyzed for lesion diameter and subtype at baseline and follow-up MRI.

Statistical analysis

Clinical, pathological and MRI data were summarized on an Excel document (Microsoft 2019 version 16.23, Redmond, WA). Categorical variables were summarized as percentage, whereas continuous variables were summarized as mean and standard deviation or median and interquartile ranges. For continuous variables, differences were evaluated with the Student *t-test* or Mann-Whitney test, as appropriate. For categorical variables, differences were tested using either the $\chi 2$ test, Fisher's exact test or McNemar test, as appropriate. Median time of follow-up were compared using Kruskal-Walles test.

First, we analyzed multiple patient and lesion characteristics – including sex, age, and lesion subtype in the overall study cohort. Then, we divided all patients into two groups according

to the number of lesions: solitary HCA or multiple HCAs. We analyzed and compared clinical features, lesion size at baseline and follow-up MRI exams, as well as pathological characteristics of the lesions and of the non-tumoral liver parenchyma between the two groups. Of note, except for demographics, other clinical variables were available only in the 95 (80.5%) of 118 patients who joined for the telephone interview and the predictive role was analyzed within these patients only (further information on missing data are in the **Supplementary Data**).

Long-term evolution of patients with HCAs was analyzed first on a per-patient basis (solitary HCA vs. multiple HCAs groups) and then on a per-lesion basis and these analyses were aimed at identifying clinical, pathological or imaging variables predictive of HCA progression (progressive disease patients vs. patients without progressive disease) as further detailed in **Supplementary Data** [22-24].

Statistical analyses were performed with the Statistical Package for the Social Sciences software, version 20.0 (SPSS Inc., Chicago, IL) or using the R computing platform (www.r-project.org). All p values were two-tailed. Statistical significance was set at $p < 0.05$.

2.3 Results

Study Cohort: Clinical and Pathological Data

Figure 1 portrays the patients' accrual flowchart. One-hundred-forty-five patients were excluded for the following reasons: (a) preoperative or follow-up MRI was not available – including lack of a minimum overall follow-up of 6 months (n=107); (b) presence of hepatic malignancies (e.g. HCC, metastases) (n=13); (c) patients treated with locoregional therapies (i.e. transarterial embolization, radiofrequency ablation) or transplantation, and lack of pretreatment MRI follow-up ≥ 6 months (n=22); (d) inadequate MRI protocol (n=3).

The final study cohort consisted of 118 patients (mean age, 40 ± 10 years; 10 men and 108 women), including 41 patients with a solitary HCA (40 ±14 years; 5 men and 36 women) and 77 patients with multiple HCAs (40 ±10 years; 5 men and 72 women). Overall, 338 HCAs (mean diameter at diagnosis [SD], 3.8 ± 3.3 cm) were analyzed in this study at baseline MRI, including 172 (50.9%) with pathology proof (i.e. 41 lesions and 131 lesions in patients with solitary and multiple HCAs, respectively) and 166 (49.1%) without pathology confirmation. The telephone interview could be performed in 95 (80.5%) of 118 patients; therefore, some of the clinical information were available and analyzed for these 95 patients. The characteristics of the study cohort are summarized in **Table 1**. The only significant differences in clinical and imaging characteristics between solitary and multiple HCAs cohorts were the duration of oral contraception intake before diagnosis of HCA, which was lower for patient with solitary HCAs (mean [SD] 12.4 years ± 7.8 vs. 17.7 years ± 9.5; p = 0.003), and lesion size at diagnosis and follow-up which was larger for solitary HCAs (mean

diameter at diagnosis [SD], 6.1 cm ± 3.7 vs. 3.5 cm ± 3.1; $p < 0.001$; mean diameter at follow-up [SD], 5.9 cm ± 3.6 vs. 2.2 cm ± 2.5; $p < 0.001$).

Inflammatory, HNF-1α inactivated and ß-catenin mutated exon 3 or exon 7-8 HCAs were encountered in 64/118 (50.8%), 46/118 (39.6%) and in 7/118 (5.9%) patients, respectively (**Supplementary Table 1)**. Eight (6.8%) of 118 patients had two different subtypes of HCAs – including four patients with inflammatory and HNF-1α inactivated HCAs, two patients with inflammatory and ß-catenin mutated HCAs, one patient with inflammatory and unclassified HCAs, and one patient with HNF-1α inactivated and ß-catenin mutated HCAs (**Supplementary Table 2**).

Intratumoral hemorrhage and malignancy were encountered at pathology in 29.7% (35 of 118) and 5.9% (7 of 118) of the patients, respectively. Foci of malignancy developed among ß-catenin mutated HCAs in five of seven (71.4%) patients with ß-catenin mutation –four with ß-catenin mutation in exon 3 and one with ß-catenin mutated in exon 7-8 HCA –, and two of 64 (3%) patients with inflammatory HCAs. None of the HNF-1α inactivated HCAs in our cohort showed malignancy at pathology at baseline.

In a per lesion analysis, the 44 HCAs with micro- and/or macroscopic hemorrhage detected at pathology corresponded to 26 of 90 (28.9%)) were inflammatory, eight of 60 (13.3%) were HNF-1α inactivated, five of six (83.3%) were sonic-hedgehog, four of six (66.7%) were ß-catenin mutated exon 3 and one of two (50%) was ß-catenin mutated exon 7-8 HCAs. None (0%) of the six unclassified HCAs showed micro- and/or macroscopic hemorrhage at pathology.

Solitary and Multiple Adenomas: Long-Term Evolution

Median follow-up – calculated from baseline MRI to last available follow-up MRI – of the entire study cohort was 5 years (IQR: 3.0 – 7.5), and it was not different between the solitary and multiple HCAs cohorts (5.1 years (IQR: 3.4-8.3 years) vs. 4.9 years (IQR: 3.0-7.3 years), respectively, p = 0.62).

Thirty-seven (90.2%) of 41 solitary HCAs and fifty-five (71.4%) of 77 patients with multiple HCAs showed stable or regressive disease (**Figure 2** and **3**, **Table 2**). Consequently, 22 (28.6%) of 77 patients with multiple HCAs showed progressive disease – including 12 (54.5%) with at least five lesions at baseline and one (4.5%) with malignancy at pathology. Overall, new lesions were identified at follow-up in two (4.9%) of 41 patients with solitary adenomas, in 12 (15.6%) of 77 patients with multiple HCAs (p= 0.087).

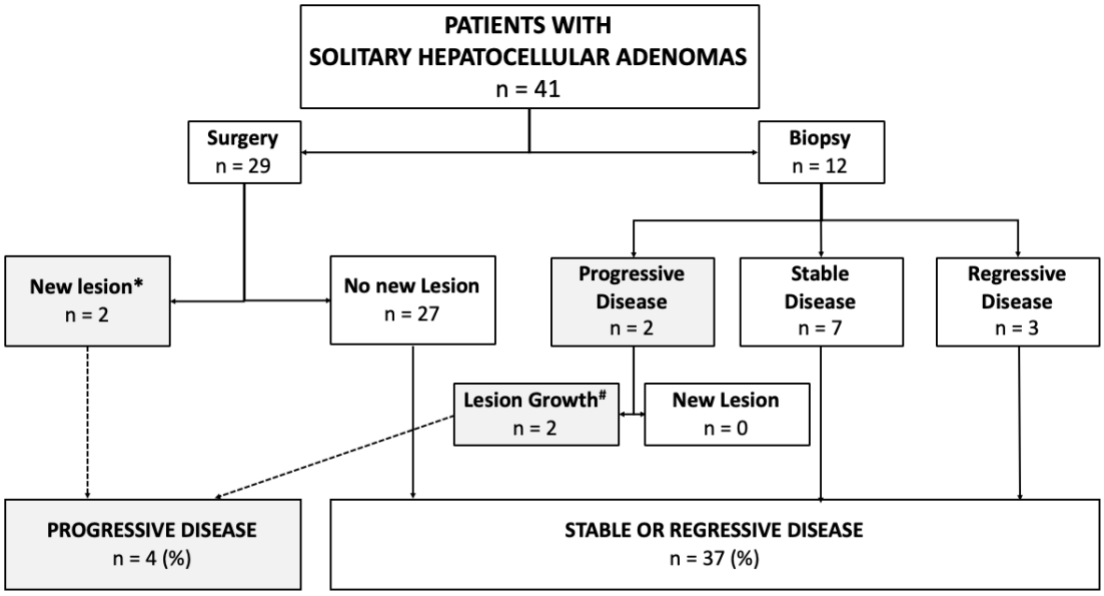

** patient 1: inflammatory HCA with signs of malignancy; patient 2: ß-catenin activated HCA*
 # patient 1: HNF-1α mutated HCA; patient 2: inflammatory HCA – history of tamoxifen intake for breast cancer

Fig. 2 – Long-term evolution of histologically proven solitary hepatocellular adenomas, by pathology proof.

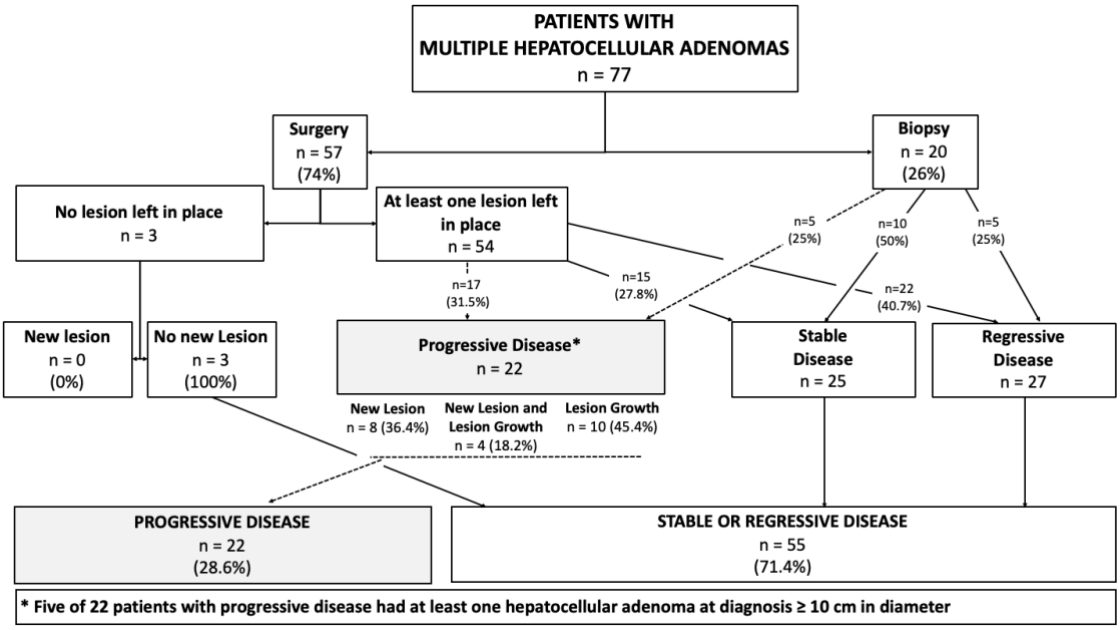

Fig. 3 – Long-term evolution of histologically proven multiple hepatocellular adenomas, by pathology proof.

In the cohort of patients with solitary lesions, inflammatory HCAs, HNF-1α inactivated HCAs and ß-catenin mutated exon 3 showed progression in two of 20 (10%), one of 15 (6.7%) and one of three (33.3%) patients, respectively. Of the 29 patients with resected solitary adenomas, only two (6.9%) showed progressive disease and both of them had at-risk HCAs (one ß-catenin mutated in exon 3 and one inflammatory HCA with foci of malignancy) (**Figure 2**); conversely, of the 12 patients with solitary HCAs not resected only two (17%) had progression because of lesion growth. In the cohort of patients with multiple HCAs of a single subtype, only inflammatory HCAs and HNF-1α inactivated HCAs showed progression

in seven of 37 (18.9%) patients and in 11 of 26 (42.3%) patients, respectively.

Representative images of long-term follow-up of inflammatory HCAs and HNF-1α inactivated HCAs are shown in **Figures 4 and 5**, respectively.

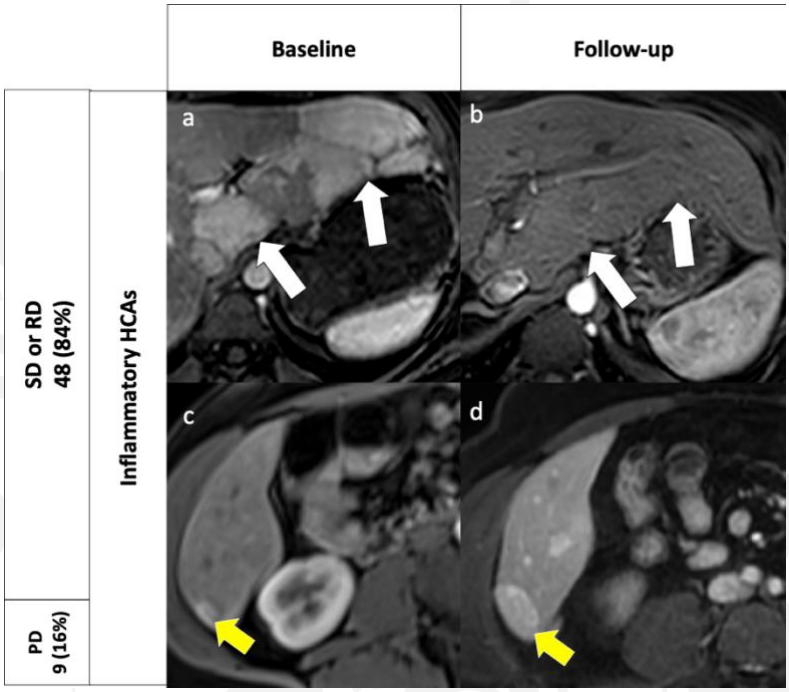

Fig. 4 – Representative images of size changes of inflammatory hepatocellular adenomas. Outcome of patients with only inflammatory hepatocellular adenomas in our study is also represented in number and percentages on the left. Top row: 30-year old woman with hepatocellular adenomas; axial contrast-enhanced MRI images at baseline (a) and at 4-year follow-up (b) demonstrate substantial regression of inflammatory hepatocellular adenomas (white arrows). Bottom row: 41-year old woman with hepatocellular adenomas; axial contrast-enhanced MRI images at baseline (c) and at 6-years follow-up (d) demonstrate a substantial progression of an inflammatory hepatocellular adenoma (yellow arrows).

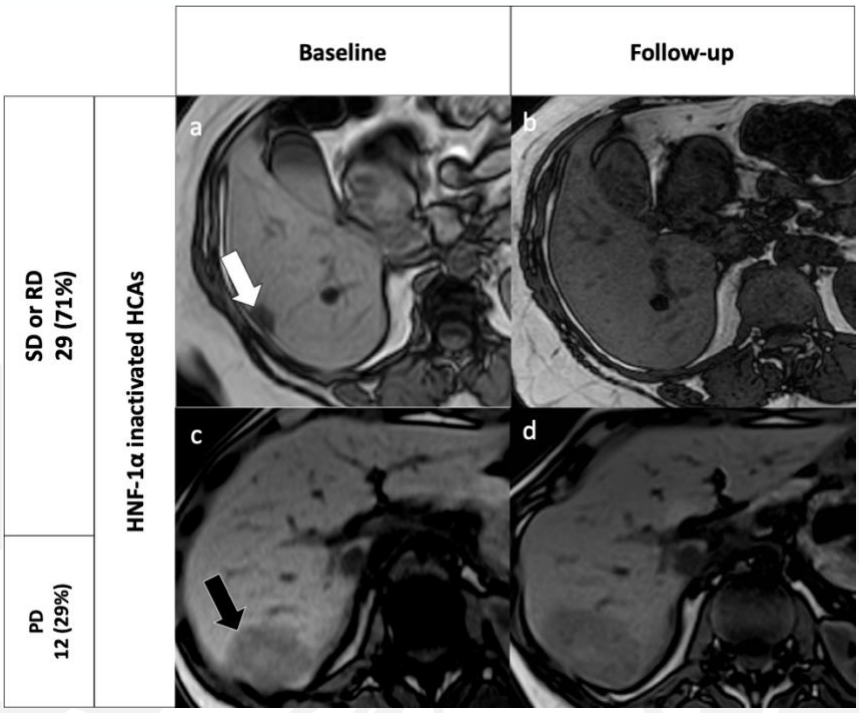

Fig. 5 – Representative images of size changes of HNF-1α inactivated hepatocellular adenomas. Outcome of patients with only HNF-1α inactivated hepatocellular adenomas in our study is also represented in number and percentages on the left. Top row: 47-year old woman with hepatocellular adenomas; axial contrast-enhanced MRI images at baseline (a) and at 12-year follow-up (b) demonstrate a complete regression of an HNF-1α inactivated hepatocellular adenoma (white arrow). Bottom row: 42-year old woman with hepatocellular adenomas; axial contrast-enhanced MRI images at baseline (c) and at 5-year follow-up (d) demonstrate a substantial progression of an HNF-1α inactivated hepatocellular adenoma (yellow arrows).

Only one (33.3%) of the three patients with at least one ß-catenin mutated HCA showed progressive disease in the long-term follow-up (**Supplementary Table 2**). The long-term evolution in men (10/118 patients) with HCAs included progressive disease in 4 of 10 patients (40%) (**Supplementary data)**.

Figure 6 summarizes long-term follow-up of HCAs according to lesion management: new lesions were observed only in two (6%) of 32 patients who underwent complete resection of HCAs, while progressive disease was demonstrated in 17 (31%) of 54 and seven (22%) of 32 patients who had partial resection or no resection, respectively. Specifically, of the 77 patients with multiple HCAs (**Figure 3**), three (5.3%) underwent complete resection of HCAs and in none of these three patients new lesions occurred at follow-up; the remaining 74 patients with multiple HCAs included 54 patients with incomplete resection and 20 patients with no surgery at all, and progressive disease was detected in 17 (31.5%) of 54 patients (i.e. eight with lesions growth only, seven with new lesions, and two with lesions growth and new lesions) and five (25%) of 20 patients (i.e. two with lesion growth, one with new lesion,

and two with both lesions growth and new lesion), respectively.

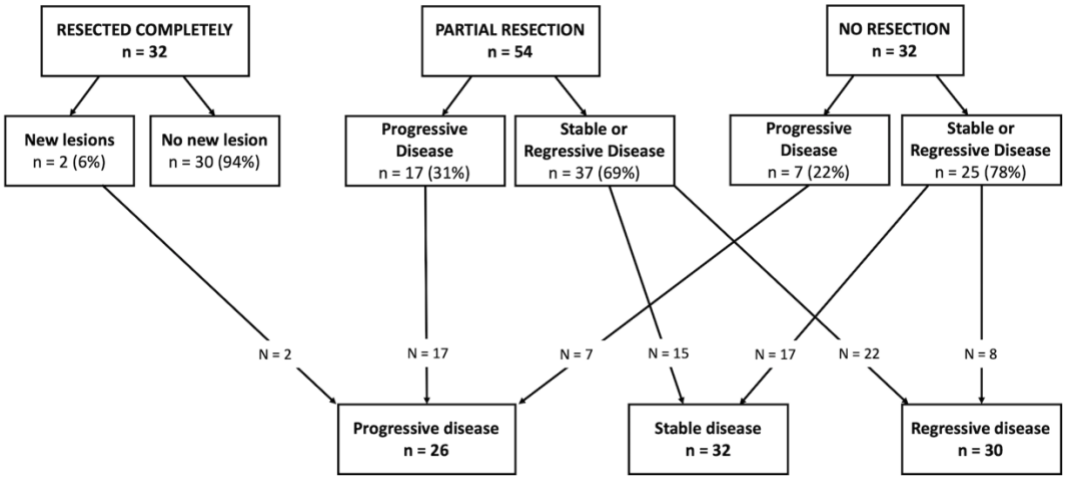

Fig. 6 – Long-term evolution of histologically proven hepatocellular adenomas, by patient management.

Overall, seven HCAs initially < 50 mm in five patients progressed to a ≥ 50 mm diameter at overall follow-up. These seven lesions that progressed over 50 mm diameter included one lesion in a patient with a solitary non-resected HNF-1α inactivated HCA, three lesions in one patient with multiple HNF-1α inactivated HCAs, two HNF-1α inactivated HCAs in two patients, and one inflammatory HCA in the remaining patient. None of our patients had malignant transformation of HCAs during follow-up, including HCAs that increased in size. None of our patients experienced clinically relevant bleeding of their HCAs.

Predictive variables of progression

Neither surgery nor presence of ß-catenin mutated subtype had an impact on progression (p = 0.99, p = 0.67) (**Table 3**), while lower BMI at diagnosis, symptoms at diagnosis, and

presence of multiple HCAs were associated with higher probability of progressive disease at univariate analysis (p = 0.001, p = 0.04, and p = 0.02, respectively) and at multivariate analysis (p = 0.006, p = 0.01 and p = 0.05). However, the number of lesions at diagnosis in patients with multiple HCAs was not associated with progressive disease (p = 0.54). Overall, inflammatory HCAs showed a significantly greater reduction in size compared to HNF-1α inactivated HCAs (**Figure 7, Table 4 and Supplementary Figure 1**), while baseline diameter was not significantly correlated with size changes (r = -0.01). Finally, in a per-lesion analysis when using a cut-off of 20% for defining progression of each lesion, 23 (27%) of 85 HNF-1α inactivated HCAs, 13 (13%) of 103 inflammatory HCAs showed progression, and none of the HCAs within the remaining subtypes showed progressive disease. The risk of progression of HNF-1α inactivated HCAs was greater – though marginally – compared to the remaining subtypes (non-HNF-1α inactivated HCAs vs. HNF-1α inactivated HCAs: OR:0.20, p=0.05). Of note, none of the 11 patients with unclassified, sonic hedgehog, or ß-catenin mutated in exon 7-8 HCAs showed progressive disease. Among patients with multiple HCAs of a unique subtype only, HNF-1α inactivated HCAs showed a higher rate of progression compared to inflammatory HCAs (11/26 [42.3%] vs. 7/37 [18.9%], p=0.04) (**Table 5**) in a similar median follow-up (5.5 years [IQR: 3.8-7.7 years] vs. 5.25 years [IQR: 2.9-7.2 years], respectively; p = 0.17), lower use and lesser duration of oral contraceptives intake (28/32 [87.5%] vs. 45/45 (100%), p=0.03, and mean 12.0±7.5 years vs. 19.2±9.2 years, p = 0.001, respectively).

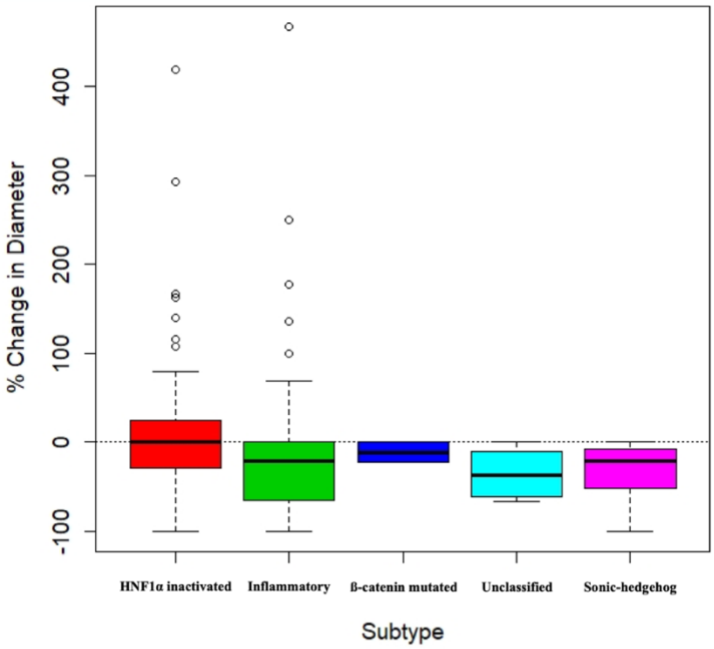

Subtype of HCA	1st quartile	Median	3rd quartile	Mean
HNF1α inactivated	-29	0	25	5.67
Inflammatory	-65.5	-21	0	-21.39
ß-catenin mutated	-17.25	-11.5	-5.75	-11.50
Unclassified	-57.5	-37	-15	-35.50
Sonic-hedgehog	-44.25	-21	-12.75	-33.0

Fig. 7 – Boxplots showing distribution of change in lesion diameter in percentage (baseline MRI exam at diagnosis to last available MRI exam) by subtype, mean, median, first and third quartiles of changes in percentages by subtype.

2.4 Discussion

Current EASL guidelines recommend continued surveillance with MRI for patients diagnosed with HCAs [1]. However, to date there are few studies that provide evidence on the natural history of HCAs on MRI. The studies that do exist were limited by short/mid-term follow-up, use of combined diagnostic criteria – including imaging and/or pathology, and the lack of use of MRI for follow-up [8-16]. Our study – which analyzed the MRI long-term course of HCAs in pathology-proven and subtyped solitary and multiple HCA– demonstrated that 90% of patients with solitary HCAs and 71% of patients with multiple HCAs show stability or regression in size after oral contraception withdrawal at a median MRI follow-up of 5 years. We also demonstrated that multiplicity of the lesions and HNF-1α inactivated subtype are significantly (p=0.02 and p=005, respectively) associated with progression. Additionally, surgery does not significantly change progression rate in patients with multiple HCAs (p=0.18).

The proportion of patients with progressive disease in the literature has varied from 0% to 19% [6-16]. A recent study by Shao N et al [25] has reported stability or regression in size in 95% of HCAs at an average follow-up of 43 months, which is slightly different compared to our rates of regression or stability (71%-90%). However, these differences may be explained by the different definition of significant reduction in size (at least 20% decrease in size compared to at least 30% decrease in size in our study), the inclusion of more than three lesions per patient (in our study we analyzed no more than three lesions in each patient to prevent clustering bias) and by the per-lesion analysis instead of a per-patient analysis. Our results demonstrated new lesions in only 2/7 (7%) of patients with resected solitary HCAs

and both these patients had at-risk HCAs at baseline pathology– including HCA with presence of ß-catenin mutation in exon 3 or foci of malignancy on resected tumor. Conversely, patients with solitary resected HCA without such worrisome features at pathology did not show new lesions after a median follow-up of 5.1 years. Therefore, our data may suggest that after resection of solitary HCAs, follow-up should be maintained in ß-catenin mutated HCAs or in the presence of foci of malignancy within the resected tumor. Discontinuation of follow-up may be discussed otherwise. One prior study by Karkar et al. [12] assessed the tumor course in a cohort of 22 patients with resected solitary HCAs, demonstrating new lesions in only two patients whose resected HCA exceeded 10 cm. In our study, the rate of progression of non-resected solitary HCAs was 16% due to tumor size increase in all the patients showing progression, and therefore these patients need to be followed-up according to EASL guidelines.

Our results show that HNF-1α inactivated HCAs have a higher probability of progression compared to inflammatory HCA (42% vs. 19%, p=0.04). These results agree with a recent study by Klompenhouwer et al [26] that demonstrated that inflammatory HCA are more likely to regress at 1 and 2 years follow-up. This may be potentially explained by different levels of estrogen dependency of different HCA subtypes [4, 27]. Unfortunately, as recently pointed out by Haring et al [15], no study has, to our knowledge, performed any subtype analysis of expression of androgen and estrogen receptors. Overall, 29% of multiple HCAs showed progression in our study, with a similar percentage in the biopsy and surgery group (25% vs. 29%, p=0.184). Surprisingly, none of the patient- and lesion-related variables that have been previously reported to be risk factors for HCA appearance and progression (e.g. BMI) [14-

16, 28] were associated with tumor progression in our study. As a result, and in line with EASL guidelines [1], patients with multiple HCAs should be monitored regardless of prior surgery, patient- or lesion- variable.

Our study had several limitations. First, we had a very low number of unclassified, sonic hedgehog, or ß-catenin mutated in exon 7-8 HCAs (n = 11/118). Second, besides demographics, other clinical variables were analyzed only in the 95 (80.5%) of 118 patients that were reached for the telephone interview, thus potentially skewing our results. However, telephone interview is considered an effective method of data collection [29]. Third, due to the retrospective nature of our study the lack of serial MRI exams did not allow for the analysis of the time to progression or valid assessment of tumor volume doubling times, and therefore the identification of the best time-points for MRI follow-up. Fourth, due to our stringent inclusion criteria, we excluded 145 patients which could lead to selection bias. However, our aim was to fill the current need for robust data on long-term evolution of path-proven HCAs using MRI as the reference standard. We also acknowledge that we did not collect data regarding changes of MRI signal features over time – including occurrence of hypersignal on T1-weighted during follow-up that could correspond to hemorrhage – because this was beyond the scope of the study. However, no clinically relevant bleeding was identified during patient follow-up. Similar findings have been described in prior literature [4,5] – including one study on MRI performed by our team [19]. Finally, RECIST 1.1 assessment of patient outcome as progressive, stable, or regressive disease is not validated for benign liver diseases. However, RECIST 1.1 is the most known, widely

adopted, and reproducible system in the oncologic setting, and it has been used in a very recent study [15].

In conclusion, our data suggest that in patients with solitary HCA, surveillance may be potentially discontinued after resection, except in ß-catenin mutated HCAs or foci of malignancy within the resected tumor. Our data also show that patients with multiple HCAs are more likely to have progressive disease regardless of surgery, with HNF-1α inactivated HCAs being the most common subtype showing progression. The lower exposure to oral contraceptives in patients with HNF-1α inactivated HCAs compared to inflammatory ones suggests the presence of other possible influencing factors for the development and progression of these lesions. Further studies analyzing changes in MRI signal features over time and other possible influencing factors of progression in patients with multiple HCAs are needed.

2.5 References

1. European Association for the Study of the Liver (EASL) EASL Clinical Practice Guidelines on the management of benign liver tumours. J Hepatol 2016; 65:386–398.

2. Bonder A, Afdhal N. Evaluation of liver lesions. Clin Liver Dis 2012;16: 271–283.

3. Karhunen PJ. Benign hepatic tumours and tumour like conditions in men. J Clin Pathol 1986; 39:183–188.

4. Nault JC, Couchy G, Balabaud C, et al. Molecular Classification of Hepatocellular Adenoma Associates With Risk Factors, Bleeding, and Malignant Transformation. Gastroenterology 2017; 152:880-894.

5. Van Aalten SM, De Man RA, Ijzermans JNM, Terkivatan T. Systematic review of haemorrhage and rupture of hepatocellular adenomas. British Journal of Surgery 2012; 99:911–916.

6. Bioulac-Sage P, Laumonier H, Couchy G, et al. Hepatocellular adenoma management and phenotypic classification: the Bordeaux experience. Hepatology 2009; 50:481-489

7.Herman P, Coelho FF, Perini MV, Lupinacci RM, D'Albuquerque LA, Cecconello I. Hepatocellular adenoma: an excellent indication for laparoscopic liver resection. HPB (Oxford) 2012;14:390-395.

8. de'Angelis N, Memeo R, Calderaro J, et al. Open and laparoscopic resection of hepatocellular adenoma: trends over 23 years at a specialist hepatobiliary unit. HPB (Oxford) 2014; 16:783–788.

9. Chun YS, Parker RJ, Inampudi S, et al. Imaging Surveillance of Hypervascular Liver Lesions in Non-Cirrhotic Patients. J Gastrointest Surg 2016; 20:564–567

10. Dokmak S, Paradis V, Vilgrain V, et al. A Single-Center Surgical Experience of 122 Patients With Single and Multiple Hepatocellular Adenomas. Gastroenterology 2009; 137:1698–1705.

11. Shafizadeh N, Genrich G, Ferrell L, Kakar S. Hepatocellular adenomas in a large community population, 2000 to 2010: reclassification per current World Health Organization classification and results of long-term follow-up. Hum Pathol 2014; 45:976-983.

12. Karkar AM, Tang LH, Kashikar ND, et al. Management of hepatocellular adenoma: comparison of resection, embolization and observation. HPB (Oxford) 2013; 15:235–243.

13 Klompenhouwer AJ, Bröker MEE, Thomeer MGJ, Gaspersz MP, de Man RA, IJzermans JNM. Retrospective study on timing of resection of hepatocellular adenoma. Br J Surg 2017; 104:1695–1703.

14. Bunchorntavakul C, Bahirwani R, Drazek D, et al. Clinical features and natural history of hepatocellular adenomas: the impact of obesity. Aliment Pharmacol Ther 2011; 34:664–674.

15. Haring MPD, Gouw ASH, de Haas RJ, Cuperus FJC, de Jong KP, de Meijer VE. The effect of oral contraceptive pill cessation on hepatocellular adenoma diameter: a retrospective cohort study. Liver Int. 2019; 39:905-913.

16. Klompenhouwer AJ, Sprengers D, Willemssen FEJA, Gaspersz MP, Ijzermans JNM, De Man RA. Evidence of good prognosis of hepatocellular adenoma in post-menopausal women. J Hepatol 2016; 65:1163–1170

17. Zulfiqar M, Sirlin CB, Yoneda N, et al. Hepatocellular adenomas: Understanding the pathomolecular lexicon, MRI features, terminology, and pitfalls to inform a standardized approach. J Magn Reson Imaging. 2019 Aug 16. doi: 10.1002/jmri.26902.

18. von Elm E, Altman DG, Egger M, Pocock SJ, Gøtzsche PC, Vandenbroucke JP; STROBE Initiative. The Strengthening the Reporting of Observational Studies in Epidemiology (STROBE) Statement: guidelines for reporting observational studies. Int J Surg 2014; 12:1495-1499.

19. Ronot M, Bahrami S, Calderaro J, et al. Hepatocellular adenomas: accuracy of magnetic resonance imaging and liver biopsy in subtype classification. Hepatology 2011; 53:1182-1191.

20. Laumonier H, Bioulac-Sage P, Laurent C, Zucman-Rossi J, Balabaud C, Trillaud H. Hepatocellular adenomas: magnetic resonance imaging features as a function of molecular pathological classification. Hepatology. 2008; 48:808-818.

21. Eisenhauer EA, Therasse P, Bogaerts J, et al. New response evaluation criteria in solid tumours: Revised RECIST guideline (version 1.1). Eur J Cancer 2009; 45:228–247.

22. Fitzmaurice G, Laird N, Ware J, Applied Longitudinal Analysis, 2nd ed, 2011 Wiley.

23. Pinheiro J, Bates D, DebRoy S, Sarkar D, nlme: Linear and Nonlinear Mixed Effects Models, R package 2019, version 3.1-141, https://CRAN.R-project.org/package=nlme

24. Bates D, Machler M, Bolker B, Walker S, Fitting Linear Mixed-Effects Models Using lme4, J. Stat. Software, 2015; 67,1, 1-48

25. Shao N, Pandey A, Ghasabeh MA, et al. Long-term follow-up of hepatic adenoma and adenomatosis: analysis of size change on imaging with histopathological correlation. Clin Radiol. 2018; 73:958-965.

26. Klompenhouwer AJ, Alblas M, Vivica van Rosmalen B, et al. Development and validation of a model to predict regression of large size hepatocellular adenoma. Am J Gastroenterol 2019 Mar 27. (https://doi.org/10.14309/ajg.0000000000000182)

27. Nault JC, Paradis V, Cherqui D, Vilgrain V, Zucman-Rossi J. Molecular classification of hepatocellular adenoma in clinical practice. J Hepatol 2017; 67:1074–1083.

28. Bröker MEE, Gaspersz MP, Klompenhouwer AJ, et al. Inflammatory and multiple hepatocellular adenoma are associated with a higher BMI. Eur J Gastroenterol Hepatol 2017; 29:1183-1188.

29. Musselwhite K, Cuff L, McGregor L, King KM. The telephone interview is an effective method of data collection in clinical nursing research: a discussion paper. Int J Nurs Stud 2007;44:1064-1070.

2.6 Tables

Table 1. Characteristics of the study population including clinical and pathological data.

Characteristics	**Solitary (41 patients)**	**Multiple (77 patients)**	**p-value**
Gender			0.31
Male	5 (12.2)	5 (6.5)	
Female	36 (87.8)	72 (93.5)	
Age (yrs) range	40 (14) 18-69	40 (10) 20-65	1.00
Telephone Interview			0.09
No n (%)	12 (29.3)	11 (14.3)	
Yes n (%)	29 (70.7)	66 (85.7)	
Height (m)	1.65 (0.06)	1.62 (0.21)	0.37
Weight (Kg)	68.3 (14.8)	72.9 (19.5)	0.19
Body Mass Index (Kg/m^2)	25 (5.3)	26.9 (7.2)	0.14
Type 2 diabetes	2 (6.9)	7 (10.6)	0.72
Hypercholesterolemia	2 (6.9)	3 (4.5)	0.64
Arterial hypertension	1 (3.4)	13 (19.7)	0.06
Symptoms at diagnosis	11 (37.9)	27 (40.9)	0.82
Oral contraception	24 (82.7)	62 (93.9)	0.13
Duration of oral contraceptive intake (yrs)	12.4 (7.8)	17.7 (9.5)	0.003
Age at menarche (yrs)	13.2 (1.98)	13 (2.0)	0.61
Menopause	12 (41.4)	25 (37.9)	0.82
Pregnancy	19 (65.5)	49 (74.2)	0.46
Pathology analysis			
Micro- and/or Macroscopic Hemorrhage	8 (19.5)	27 (35.1)	0.09
Malignancy	3 (7.3)	4 (3.1)	0.36
Non tumoral liver	***38 PATIENTS***	***57 PATIENTS***	
Fibrosis	3 (7.9)	9 (15.8)	0.35
Steatosis	14 (36.8)	32 (56.1)	0.09
Steatosis (%)	10.3 (18.1)	19.3 (26.4)	0.05
Micro-adenomas	0 (0)	13 (23.2)	0.001
Lesion Characteristics	***41 HCAs***	***297 HCAs***	
Lesion size at diagnosis (cm)	6.1 (3.7)	3.5 (3.1)	<0.001

Lesion size at diagnosis			<0.001
<5 cm	20 (48.8)	229 (77.1)	
≥5 cm	21 (51.2)	68 (22.9)	
Lesion size at follow-up MRI exam (cm)	5.9 (3.6)	2.2 (2.5)	<0.001
Variation in size diagnosis-follow-up (%)*	-6.1 (38.9)	-12 (75.6)	0.64
≤-30%	3 (16.7)	76 (36.4)	0.17
-30%-20%	12 (66.6)	95 (45.4)	
>20%	3 (16.7)	38 (18.2)	
Footnotes – Categorical variables are reported as numbers and percentages. Continuous variables are reported as mean and standard deviation. HCAs: hepatocellular adenomas SD: standard deviation; yrs: years; Min: minimum; Max: maximum.			

Table 2. Follow-up analysis of solitary and multiple adenomas in a per-patient analysis.

Characteristics	Stable disease	Progressive disease	Regressive disease	*p*-value
SOLITARY ADENOMA	5 (83.3)			
Long-term evolution				
Overall (41)	34 (83)	4 (9.7)	3 (7.3)	
Pathologic proof				0.009
Biopsy (12)	7 (58.3)	2 (16.7)	3 (25)	
Surgery (29)	27 (93.1)	2 (6.9)	0 (0)	
Size				0.71
0-5 (20)	15 (75)	2 (10)	3 (15)	
≥5 cm (21)	19 (90.5)	2 (9.5)	0 (0)	
Adenoma subtype				
Inflammatory (20)	17 (85)	2 (10)	1 (5)	
HNF-1α inactivated (15)	12 (80)	1 (6.7)	2 (13.3)	
ß-catenin mutated exon 3 (3)	2 (66.7)	1 (33.3)	0 (0)	
Unclassified (3)	3 (100)	0 (0)	0 (0)	
MULTIPLE ADENOMAS				
Long-term evolution,				
Overall (77)	26 (33.8)	22 (28.6)	29 (37.6)	
Pathologic proof				0.18
Biopsy (20)	10 (50)	5 (25)	5(25)	
Surgery (57)	16 (28.1)	17 (29.8)	24 (42.1)	
Adenoma subtype				
Unique Subtype (69)	24 (34.8)	18 (26.1)	27 (39.1)	
Inflammatory (37)	13 (35.1)	7[#](18.9)	17 (45.9	0.04
HNF-1α inactivated (26)	8 (30.8)	11* (42.3)	7 (26.9	
Unclassified (2)	1 (50)	0 (0)	1(50)	
ß-catenin mutated exon 7-8 (1)	0 (0)	0(0)	1 (100)	
Sonic Hedgehog (3)	2 (66.7)	0 (0)	1 (33.3)	
Two Subtypes (8)	2 (25)	2(25)	4 (50)	

*Of the 11 HNF-1α inactivated HCAs that progressed, 6 showed lesion growth, 2 new lesions, and 3 both lesion growth and new lesions
Of the 7 inflammatory HCAs that progressed, 2 showed lesion growth, 4 new lesions, and 1 both lesion growth and new lesions

Footnotes – *Regressive disease* is defined as a decrease in size of at least a 30% in the sum of diameters of target lesions, taking as reference the baseline sum diameters, or disappearance of all the target lesions; *progressive disease* is defined as at least a 20% increase in the sum of diameters of target lesions, taking as reference the baseline sum diameters or appearance of new lesions; *stable disease* is defined as small changes in the diameter of the target lesions that do not meet above criteria for progressive or regressive disease.
Categorical variables are reported as numbers and percentages. Continuous variables are reported as mean and standard deviation. Of note, stable and progressive disease in patients with surgically resected solitary adenomas and in patients with surgically resected multiple adenomas without any lesion left in place after surgery depends only on the lack of new lesions at post-operative MRI follow-up.

Table 3. Patient and lesion variables affective progressive disease in all patients with adenomas at univariable analysis in a per-patient analysis.

Characteristics	Progressive Disease	Lack of Progressive Disease	*p*-value
Sex			0.22
Men (10)	4 (40)	6 (60)	
Women (108)	22 (20)	86 (80)	
Age at diagnosis (yrs)	38 (10)	40 (12)	0.35
Height (m) #	1.65 (0.08)	1.63 (0.20)	0.57
Weight (Kg) #	62.3 (12.9)	73.8 (18.7)	0.01
Body Mass Index (Kg/m^2) #	23 (4)	27 (7)	0.001
Body Mass Index (Kg/m^2) rank #			0.03
<25 (49)	12 (24.5)	37 (75.5)	
25-30 (18)	6 (33.3)	12 (66.7)	
30-35 (17)	1 (5.9)	16 (94.1)	
35-40 (7)	0 (0)	7 (100)	
>40 (4)	0 (0)	4 (100)	
Type 2 diabetes #	1 (11.1)	8 (88.9)	0.68
Hypercholesterolemia #	0 (0)	5 (100)	0.32
Arterial Hypertension #	3 (21.4)	11 (78.6)	>0.99.
Symptoms #	12 (34.3)	23 (65.7)	0.04
Age at menarche (yrs) #	12 (1)	13 (2)	0.09
Menopause #	5 (13.5)	32 (86.5)	0.41
Oral Contraceptives #	16 (18.6)	70 (81.4)	0.57
Duration of Oral Contraceptives intake (yrs) #	14 (11)	17 (9)	0.20
Pregnancy #	15 (22.1)	53 (77.9)	0.55
Multiple Subtypes	3 (42.9)	4 (57.1)	0.18
Solitary vs. Multiple HCAs			0.02
Solitary (41)	4 (10.8)	37 (89.2)	
Multiple (77)	22 (28.6)	55 (71.4)	
Pathology proof			>0.99
Biopsy (32)	7 (21.9)	25 (78.1)	
Surgery (86)	19 (22.1)	67 (77.9)	

Non tumoral liver *	Overall - 21	Overall - 74	
Fibrosis	2 (9.5)	10 (13.5)	>0.99
Steatosis	9 (42.9)	37 (50)	0.63
Steatosis	18.6 (14.7)	35 (24.7)	0.14
Micro-adenomas	4 (19)	9 (12.2)	0.48
At least 1 β-catenin mutated HCA	5 (5.4)	2 (7.7)	0.67
Mean lesion size at diagnosis (cm)	6.9 (3.9)	6.1 (3.4)	0.31
Lesions at diagnosis –Multiple HCAs			0.64
2-5	11	21	
6-10	4	12	
>10	7	22	

*Characteristics of the non-tumoral liver influencing progression were evaluated only in 95 patients with available information, as detailed in the reference standard.
[#]These information were available only in the 95 (80.5%) of 118 patients that were reached for the telephone interview; percentages are only referred to data in these 95 patients.
Footnotes –*progressive disease* is defined as at least a 20% increase in the sum of diameters of target lesions, taking as reference the baseline sum diameters or appearance of new lesions. Lack of progressive disease included *stable or regressive disease*. *Regressive disease* is defined as a decrease in size of at least a 30% in the sum of diameters of target lesions, taking as reference the baseline sum diameters, or disappearance of all the target lesions; *stable disease* is defined as small changes in the diameter of the target lesions that do not meet above criteria for progressive or regressive disease. Categorical variables are reported as numbers and percentages. Continuous variables are reported as mean and standard deviation. yrs: years

Table 4. Model 1: estimated effects from mixed effects linear model of log-ratio of diameters considering all size changes by subtype in a per-lesion analysis. Model 2: Estimated effects from logistic regression of risk of progression by subtype, considering a 20% cut-off to define progressive disease of each lesion in a per-lesion analysis..

Term	Effect	Std. Error	t-value	p-value
Model 1				
Baseline (HNF-1α inactivated)	-0.2	0.17	-1.2	0.23
Inflammatory	-0.49	0.21	-2.3	0.02
ß-catenin mutated	-0.01	0.64	-0.02	0.98
Unclassified	-0.26	0.67	-0.39	0.69
Sonic hedgehog	-0.31	0.56	-0.56	0.58
Model 2	**Log-odds**	**Std. Error**	**z value**	**p-value**
Baseline (HNF-1α inactivated)	-2.53	1.34	-1.89	
Other subtypes	-1.61	0.82	-1.95	*0.05*

Footnote - **there were relatively few lesions of ß-catenin mutated, unclassified and sonic hedgehog subtypes in the dataset and in model 2 we combined inflammatory, ß-catenin mutated, unclassified and sonic hedgehog subtypes because the risk of progression for subtypes -catenin mutated, unclassified and sonic hedgehog subtypes using a 20% cut-off was 0 and this 0 value caused instability in the estimated standard errors of the effects.**

Table 5. Per-patient analysis of type of progression in patients with multiple inflammatory or HNF-1α inactivated HCAs of a unique subtype showing progressive disease at imaging follow-up.

Type of progression	**Inflammatory HCAs (37)**	**HNF-1α inactivated (26)**	***p* - value**
Progressive disease, n (%)	7 (18.9)	11 (42.3)	0.04
Lesion Growth, n (%)	2 (5.4)	6 (23.1)	0.23
New Lesions, n (%)	4 (10.8)	2 (7.7)	
Lesion Growth and New Lesions, n (%)	1 (2.7)	3 (11.5)	
Footnotes – *Progressive disease* is defined as at least a 20% increase in the sum of diameters of target lesions, taking as reference the baseline sum diameters or appearance of new lesions.			

2.7 Supplementary data file

Materials and Methods

Reference standard

In the solitary adenoma cohort, we analyzed at baseline MRI an overall of 41 hepatocellular adenomas, including 12 adenomas in the biopsy group and 29 adenomas in the surgery group. In the multiple adenomas group, we analyzed at baseline MRI an overall of 297 lesions, including 88 operated adenomas in the surgery group without any preoperative follow-up, 22 operated adenomas in the surgery group with a pre-operative follow-up MRI of at least 6 months, 128 non-operated adenomas in the surgery group with a post-operative follow-up MRI of at least 6 months and 59 adenomas in the biopsy group with a follow-up MRI of at least 6 months.

Lesion subtyping at pathology was performed according to the updated classification published by Nault et al [4] as follows: inflammatory HCA (i.e. dysregulated IL6/JAK/STAT pathway due to mutation in IL6ST, FRK, STAT3, GNAS, or JAK1, tumor overexpression of serum amyloid A and C reactive protein), HNF-1α inactivated HCA (i.e. HNF1A biallelic inactivation, decreased tumor expression of fatty acid binding protein 1), ß-catenin mutated HCA exon 3 (i.e. exon 3 CTNNB1 mutation, nuclear ß-catenin, increased glutamine synthase expression, strong ß-catenin activation), ß-catenin mutated HCA exon 7-8 (i.e. exon 7-8 CTNNB1 mutation, faint glutamine synthase expression, weak ß-catenin activation), sonic hedgehog HCA (i.e. INBHE/GLI1 fusion with sonic hedgehog activation), and unclassified HCA

MRI signal features that allowed the identification of HCA subtypes at imaging were [17]:

- Inflammatory HCA: T2 signal hyperintensity, contrast enhancement in the arterial phase which persists on portal venous and delayed phases, hypointensity on hepatobiliary phase except for some inflammatory HCAs that may show complete or partial iso- or hyperintense on hepatobiliary phase due to spontaneous hyperintensity on precontrast T1;
- HNF-1α inactivated HCA: diffuse and homogenous signal dropout on opposed phase in the dual phase T1-weighted sequence, contrast enhancement in the arterial phase which persists on portal venous and delayed phases, hypointensity on hepatobiliary phase;
- ß-catenin mutated HCA exon 3 HCA: heterogenous signal on T1-weighted and T2-weighted sequence, contrast enhancement in the arterial phase and occasionally washout on portal venous or delayed phase, iso or hyperintense signal on hepatobiliary phase;
- sonic hedgehog HCA: intrinsic hyperintensity on T1-weighted images, contrast enhancement in the arterial phase and occasionally washout on portal venous or delayed phase, hypointense on hepatobiliary phase.

Conversely, ß-catenin mutated HCA exon 7-8 and unclassified HCAs lack specific MRI features, and identification was based only on careful pathology-radiology data matching. Lesions with the same MRI imaging features (i.e. signal intensity on T1-weighted and T2-weighted imaging and post-contrast enhancement pattern) were considered as of the same molecular subtype as the pathologically proven lesion. In patients with multiple HCAs, subtyping for lesions that were chosen as target lesions but lacked pathology confirmation was based on the presence of the same imaging characteristics that were detected at

baseline MRI in the pathology-proven HCAs. The same approach was adopted for new lesions occurring at follow-up, which lacked pathology confirmation, and their subtyping was based on MRI features described above and on similarity with imaging characteristics of the pathology-proven HCAs.

MRI analysis

All patients performed MRI at both baseline and follow-ups. MRI exams included the following sequences: T2-weighted images with and without fat suppression, dual echo sequence, diffusion weighted images and apparent diffusion coefficient map, T1-weighted 3D gradient echo images precontrast, and then in the arterial, portal venous and delayed phases. If Gd-BOPTA was used as contrast agent, a hepatobiliary phase at 2 hours was also included in the protocol. Most of these MRI exams were performed at our center. MRI exams that were not performed at our center had been imported in the picture archiving and communication systems by the treating physician at the time of the visit for discussion with radiologists at multidisciplinary meetings as this is the standard-of-care at our center.

The baseline MRI exam was defined as the initial MRI exam in which the HCA was diagnosed. The preoperative MRI exam was defined as the last liver MRI exam before surgery. The follow-up MRI exam was defined as the last liver MRI exam performed.

The *target lesions* were chosen according to Response Evaluation Criteria In Solid Tumors (RECIST) version 1.1, and a maximum of three lesions per subtype per patient for follow-up evaluations were annotated at baseline in addition to the surgically resected HCAs [19]. Although RECIST 1.1 includes two lesions per organ in clinical practice, we analyzed up to

three lesions per subtype per patient to take into account subtle changes in size that may occur in benign diseases and possible presence of different subtypes, and we opted for no more than three lesions per subtype in each patient to prevent clustering bias.

For each patient, we assessed the total number of HCAs, a maximum of three target lesions per subtype per patient for follow-up evaluations at baseline MRI in addition to the surgically resected HCAs, and the longest diameter of the target lesions at baseline, preoperative, and follow-up MRI exams, according to RECIST guidelines [19]. In addition, all the MRI exams were analyzed over time to assess the appearance of new lesions. Liver adenomatosis was defined as a total number of HCAs per patient greater than 10.

The longest diameter of the lesions was measured on contrast-enhanced MRI exams including the whole lesion in the axial plane, even if on follow-up MRI exams the level or the orientation of the longest diameter of the lesion changed. Lesion size was considered as the largest outer-edge-to-outer-edge dimension of the lesion, including eventual hemorrhage within tumor. If at follow-up MRI exams, a target lesion was still visible but 'too small to measure', a default measurement of 5 mm was assigned.

Tumor measurements were used to calculate the dimensional changes at different time-points, first on a lesion-basis and then on a patient-basis. The dimensional changes were used to assess patient "outcome" according to adapted RECIST v.1.1 as follows:

-Regressive disease (RD) – which included partial or complete regression – was defined as a decrease in size of at least a 30% in the sum of diameters of target lesions, taking as reference the baseline sum diameters, or disappearance of all the target lesions;

-Progressive disease (PD) was defined as at least a 20% increase in the sum of diameters of target lesions, taking as reference the baseline sum diameters or appearance of new lesions;

-Stable disease (SD) was defined as small changes in the diameter of the target lesions that do not meet above criteria for PD or RD;

Of note, in the surgery group, follow-up was calculated from baseline MRI exam (i.e. MRI at diagnosis before surgery) to follow-up MRI exam defined as the last postoperative liver MRI exam performed by the patient. Follow-up analysis in the surgery group with complete resection of all HCAs depended only on the appearance of new lesion after surgery. In non-operated patients, follow-up was calculated from baseline MRI exam (i.e. MRI at diagnosis before surgery) to last available follow-up MRI exam.

For lesion size at diagnosis and at follow-up MRI, a cut-off of 50 mm was considered to investigate how many HCAs initially < 50 mm progressed to a ≥ 50 mm diameter at overall follow-up. A cut-off diameter of 50 mm is considered of utmost importance for indication to surgery [1].

Statistical analysis

Missing data

Clinical variables collected through telephone variables – i.e. symptoms at diagnosis, height and weight at diagnosis, diabetes, hypercholesterolemia, arterial hypertension, use of oral contraceptives, age of menarche, menopause, and history of pregnancies – were not

available in the 23 patients that we could not be contacted. Therefore, except for demographics, clinical variables predictive of progression were analyzed in the 95 (80.5%) of 118 patients that were reached for the telephone interview. Age of menarche was also not reported in one patient because she had a history of amenorrhea. Pathological information regarding the non-tumoral liver were missing in 23 of 32 patients who underwent biopsy. If one or more data was missing, the valid percentages in the available data were calculated. Indeed, these data were missing completely at random or just missing at random (i.e. patient not joined on the phone for the telephone interview because they changed home or phone number, pathological data on non tumoral liver parenchyma was not always available in the biopsy group because in some cases biopsy of the lesion only was performed).

Predictive variables of progression: per-patient and per-lesion analysis

Long-term evolution of patients with HCAs was analyzed first on a per-patient basis. Median follow-up with 1st and 3rd interquartile ranges was calculated in the overall study cohort and in the solitary HCA or multiple HCAs groups. Per each of these two groups, the outcome referred as stable-, progressive-, or regressive disease was analyzed and compared according to pathologic proof (i.e. biopsy vs. surgery), lesion size, and lesion subtype. In patients with multiple HCAs, we differentiated patients with a single subtype from those presenting with two different subtypes based on pathology. In patients with multiple HCAs, HCA subtyping was based on the similarities of imaging features with the biopsied or resected lesions. Among the patients with multiple HCAs of a single subtype, we compared

the long-term evolution and median survival between patients with inflammatory and HNF-1α inactivated HCAs.

Our final analysis was aimed at identifying clinical, pathological or imaging variables predictive of HCA progression (progressive disease patients vs. patients without progressive disease). We analyzed and compared clinical, imaging and pathological variables between patients showing progressive disease and patients without progressive disease at univariate analysis. Of note, except for demographics, other clinical variables were available only in the 95 (80.5%) of 118 patients joined for the telephone interview and the predictive role was analyzed within these patients only. A multivariate analysis was performed using a binary regression model including statistically significant variables at univariate analysis. Age at menarche was available for 37 patients only and therefore was not included.

Finally, a per-lesion analysis was performed in the overall study cohort. A scatter plot was created per each HCA subtype to investigate the entity of size changes based on the initial lesion size. Then, the distribution of size changes in percentage for the different subtypes was analyzed with change distribution centered at 0, no change. However, considering the presence of a few large positive outliers for HNF-1α inactivated and inflammatory HCAs, suggesting a positively skewed distribution of the % change, we choose to model the log-ratio (LR) of diameters, ie, LR = log((Final Dia + 0.5) Baseline Dia), where 0.5 is added to add final diameters to avoid taking log of 0. Note that the log-ratio is also a measure of change of diameter, but on a different scale to take care of skewness in the data distribution. To analyze if the differences between subtypes were statistically significant, we fit a mixed effects linear model of the form:

$LR_{ijk} = \mu + \alpha_j + b_i + \varepsilon_{ijk}$ (Model1),

where the response was the log-ratio of diameters for the k-th lesion of the j-th subtype (j = 1,…,5) in the i-th patient (i = 1,…,207). Model 1 explains variation in the log-ratio in terms of a baseline mean value □, which represents the mean change in a lesion of subtype 1, an effect of the j-th subtype , an effect for the i-th patient, b_i, which is assumed to have a zero mean Gaussian distribution and a measurement error term , which is also assumed to have a zero mean Gaussian distribution, but independent of the patient effect. Model 1 was fit to the data by the method of restricted maximum likelihood [20] using the nlme package in the R computing platform [21]. We also added the baseline diameter as a further predictor in the model. Finally, considering the presence of a cluster of lesions with large negative residuals of model 1, we tested the sensitivity of our conclusions by excluding these lesions from our analysis and the conclusions of this model (i.e. statistical significance of effects) were unchanged. Furthermore, we used a 20% cut-off to define progression for each the lesion, and we analyzed the risk of progression using a logistic regression model with a random effect for patient (similar to the one for change in diameter), as follows:

(Model 2)

Where the response is the log-odds of progression, i.e. p_{ijk} is the risk of progression for the *k*-th lesion of the *j*-th subtype (*j* = 1,…,5) in the *i*-th patient (*i* = 1,…,207). Model 2 explains variation in the log-odds in terms of a baseline mean value □, which represents the mean change in a lesion of subtype 1, an effect of the *j*-th subtype , an effect for the *i*-th patient, b_i, which is assumed to have a zero mean Gaussian distribution. Model 2 is fit to the data by the method of maximum likelihood [20] using the lme4 package in the R computing platform

[22]. Finally, we investigated any difference in the role of oral contraceptive between patients with inflammatory and HNF1α inactivated HCAs. For this analysis, we included all target lesions in women who had completed the telephone interview.

Results

Subtypes of HCAs in patients with adenomatosis

In 29 patients with adenomatosis (at least 10 HCAs), HCA subtyping included 14 patients with inflammatory HCAs, 10 with HNF-1 α inactivated HCAs, 1 with sonic hedgehog HCAs, 1 with unclassified HCAs and 3 patients with two different subtypes of HCAs.

Subtypes of HCAs and long term evolution in men with HCAs

In the 10 men with HCAs included in the final study cohort, 5 had a solitary HCA and 5 multiple HCAs. In these 10 patients, HCA subtyping included 4 patients with inflammatory HCAs, 3 with HNF-1 α inactivated HCAs and 3 with ß-catenin mutated HCA exon 3. All 10 patients except one were surgically resected for HCAs. Long-term evolution in these 10 patients included progressive disease in 4 (40%), stable disease in 4 (40%) and regressive disease in 2 (20%). Progressive disease occurred in 1 patient with solitary inflammatory HCA with foci of malignancy within the lesion at pathology, and in 3 patients with multiple HCAs including 1 patient with inflammatory HCAs, 1 patient with HNF-1 α inactivated HCAs and 1 with ß-catenin mutated HCAs exon 3.

Supplementary Table 1. Subtypes of hepatocellular adenomas in the study cohort, according to the reference standard.

	Overall study cohort (n = 118)	***Solitary HCA (n = 41)***	***Multiple HCAs (n = 77)***	
Hepatocellular Adenoma subtype	***Single subtype in 110 patients + Two Subtypes in 8 patients (n = 126)***	***Solitary HCA (n = 41)***	***Single Subtype in 69 patients (n = 69)***	***Two Subtypes in 8 patients (n = 16)***
Inflammatory	64 (50.8)	20 (48.8)	37 (53.4)	7 (43.8)
HNF-1α inactivated	46 (36.5)	15 (36.6)	26 (37.7)	5 (31.2)
Unclassified	6 (4.8)	3 (7.3)	2 (2.9)	1 (6.2)
ß-catenin mutated in exon 3	6 (4.8)	3 (7.3)	0 (0)	3 (18.8)
Sonic Hedgehog	3 (2.4)	0 (0)	3 (4.3)	0 (0)
ß-catenin mutated in exon 7-8	1 (0.8)	0 (0)	1 (1.4)	0 (0)
Footnotes – Categorical variables are reported as numbers and percentages in parenthesis; of note, percentages are calculated based on the overall number of lesions. HCA: Hepatocellular Adenoma.				

UNIVERSITÀ DEGLI STUDI DI PALERMO

Université de Paris

Supplementary Table 2. Long term evolution of patients with two different subtypes of hepatocellular adenomas

	Inflammatory HCA		**HNF-1α inactivated HCA**		**Unclassified HCA**		**ß-catenin mutated HCA**		**Overall**
Patient	Yes/ No	Follow-up	Yes/ No)	Follow-up	Yes /no	Follow-up	Yes/no	Follow-up	Follow-up
Pt 1	Yes	PD	Yes	SD	-	-	-	-	PD
Pt 2	Yes	No*	Yes	RD	-	-	-	-	RD
Pt 3	Yes	No*	Yes	RD	-	-	-	-	RD
Pt 4	Yes	PD/RD	-	-	Yes	-	-	-	SD
Pt 5	Yes	RD	-	-	-	-	Yes	No*	RD
Pt 6	-	-	Yes	SD	-	-	Yes	No*	SD
Pt 7	Yes	PD	-	-	-	-	Yes	No*	PD
Pt 8	Yes	RD	Yes	No*	-	-	-	-	RD
Total	7	-	5	-	1	-	3	-	

*** "No" in the follow-up column indicates that after surgery, no HCAs of that particular subtype was left in place and therefore an imaging follow-up was not available. HCA: hepatocellular adenoma; PD: progressive disease; SD: stable disease; RD: regressive disease**

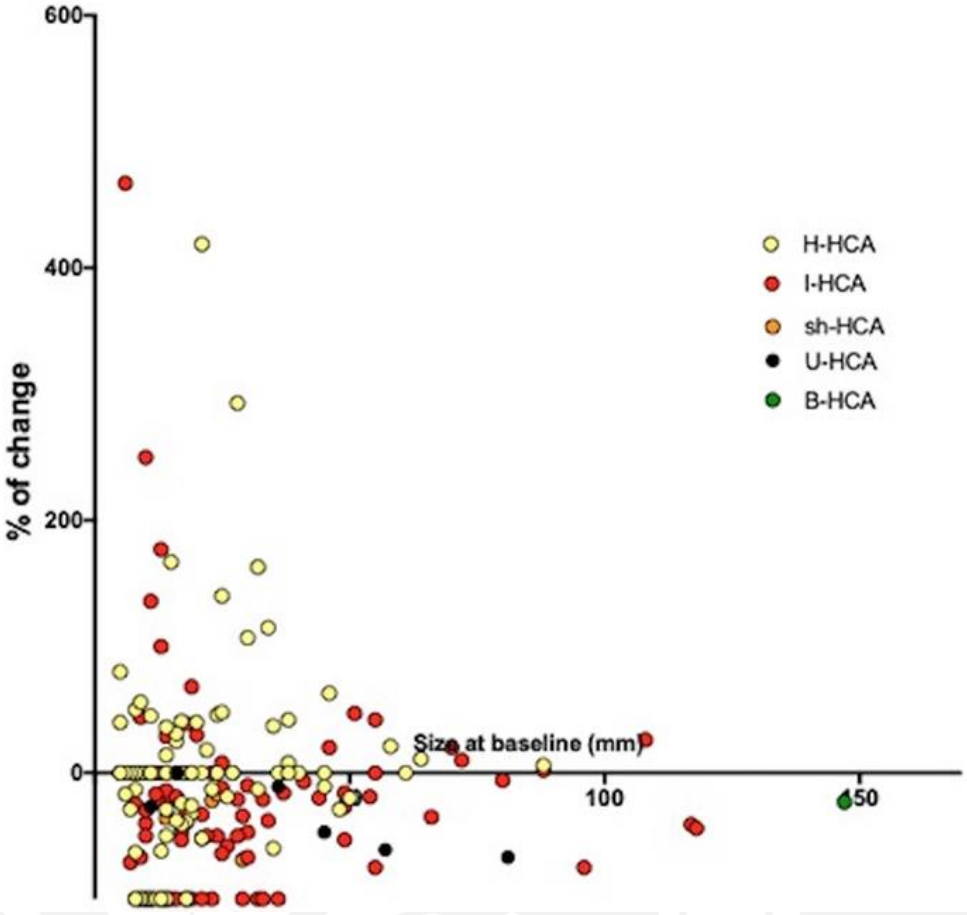

Supplementary Fig. 1 – Scatter plot showing per-lesion analysis of changes in size in percentage of hepatocellular adenomas from size at baseline by lesion subtype in the overall study cohort.